Friction and Wear of Langmuir-Blodgett Films Observed by Friction Force Microscopy

E. Meyer, R. Overney, D. Brodbeck, L. Howald, R. Lüthi, J. Frommer, and H.-J. Güntherodt

Institut für Physik, Universität Basel, Klingelbergstrasse 82, 4056 Basel, Switzerland

Lubrication is documented on a microscopic scale with a friction force microscope. A reduction in friction is observed for Langmuir-Blodgett film-covered surfaces, compared to the bare substrates. Film defects not detected in the topographic mode are clearly recorded in the friction force mode. With applied forces over 10 nN, the initial stages of wear are observed. Small islands of bilayer height are moved in their entirety, conserving the normal orientation of the aliphatic chains. This collective motion of molecules allows the shear strength of the films to be determined. The observed ability of the molecules to remain in the ordered state illustrates one of the fundamental origins of boundary lubrication.

PACS numbers: 62.20.−x

In tribology Langmuir-Blodgett films are used as model systems for boundary lubrication. Friction on metals is reduced by a factor of 10 and wear by a factor of 10000 or more [1,2]. Scanning probe microscopes, such as the atomic force microscope (AFM) [3,4] and the friction force microscope (FFM) [5], offer the opportunity to examine phenomena such as friction and wear on a local scale.

The first observation of friction with a force microscope [6] showed that frictional forces between a tungsten tip and graphite vary with the atomic periodicity of the underlying graphite surface. Frictional forces were found to increase linearly with increasing load and a friction coefficient of 0.01 was determined. The contact region was interpreted to be several thousands of atoms, producing atomic scale features from a certain degree of commensurability between the tip and sample. Recently, the anisotropy of frictional forces between muscovite mica sheets was investigated by FFM and surface force apparatus (SFA) [7]. This anisotropy was also attributed to the commensurability between the two contacting surfaces. In this study a frictionless state was postulated for the limit of complete incommensurability. In order to understand the origins of friction and wear on the nanometer scale, several models based upon *ab initio* calculations [8] and molecular dynamics calculations [9] have been introduced. These initial computational approaches have produced values for friction in agreement with the above FFM measurements on graphite [8]. They have also modeled the phenomenon of plastic deformation of surfaces under the AFM probe [9]. However, the particular case of boundary lubrication as probed by the AFM and FFM has yet to be described on a fundamental theoretical basis.

AFM measurements on Langmuir-Blodgett (LB) films have shown that molecular resolution can be achieved [10,11]. From both force-distance curves [12] and the atomic scale imaging, it is concluded that the contact region is of the order of several square nanometers. The subject of this paper is to study lubrication on a microscopic scale and to examine the initial stages of wear on Langmuir-Blodgett films as they arise in this submicron regime.

The friction studies are carried out in the following manner: One- and two-bilayer films of Cd arachidate are transferred to hydrophobized silicon wafers by standard LB techniques [13]. The films are studied with a FFM where both the normal and the lateral forces acting on the probing tip are measured simultaneously [5]. The bending and torsion of a cantilever-type spring are measured by laser-beam deflection and calibrated as described elsewhere [14–16]. The angle resolution of the position sensitive detector (PSD) is 10^{-7} rad which allows the measurement of 0.1 Å in the normal direction and 10^{-10} N in the lateral direction. Microfabricated rectangular Si_3N_4 levers with normal spring constants of 0.1–0.2 N/m and torsion spring constants of 100–200 N/m are used. The maximum adhesive forces are determined to be 3–6 nN from force-distance curves. In the Johnson-Kendall-Roberts (JKR) model [17] the work of adhesion, γ, is related to the adhesive force F_{adh} by $\gamma = 2F_{adh}/3\pi R$. With a tip radius R of 20 nm, determined from the resolution at step edges, the work of adhesion γ is 0.03–0.06 N/m, which is in agreement with the values derived from nanoindenter experiments [18]. With applied forces between 1 and 20 nN approximate contact pressures of 10–200 MPa are derived.

The examined films are found to be ∼95% homogeneous with continuous flat planes over several microns in dimension [10]. For the present study, the edges of these planes are investigated where several levels of the film and the substrate are revealed. Figure 1(a) shows a scan area representative of many consistent measurements on films of both one- and two-bilayer height. Surfaces at three levels are observed, corresponding to substrate, first bilayer, and second bilayer. The imaged surfaces of the first and second bilayers are measured as being 54 and 108 Å above the silicon surface, respectively, consistent with the expected dimensions of these cadmium arachidate LB films [10].

The reduction in friction on the film-covered surface compared to the exposed substrate is evident in the lateral force measurements, Fig. 1(b). With an applied normal force of 4 nN during scanning, the frictional force on the substrate is found to be 3 nN. On areas that are covered with the organic film, the same applied normal force re-
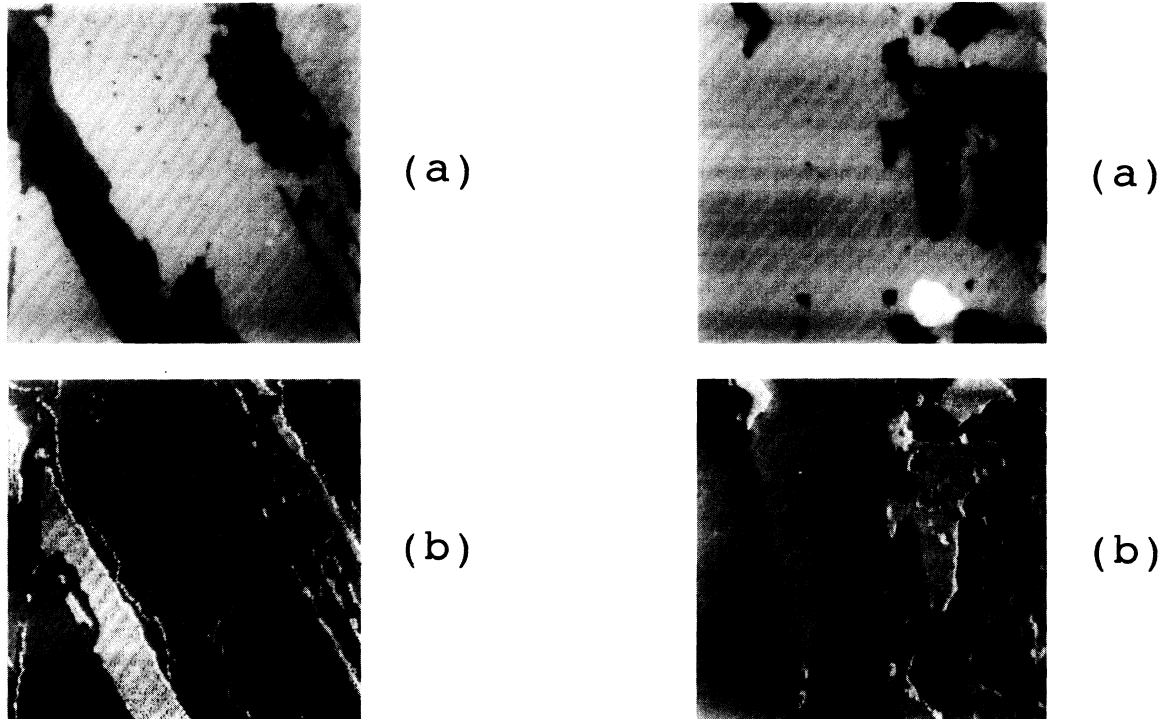
FIG. 1. FFM of a double bilayer of Cd arachidate (2×2 μm), acquired with an applied load of 4 nN. (a) Topography of the film shows one- and two-bilayer steps, each bilayer with a height of 54 Å. The lowest level corresponds to the substrate. Total vertical range is 240 Å. (b) Friction force map shows increased friction on the substrate compared to the organic film. Total range in friction force in the map is 14 nN. No difference in friction is measurable between the single- and double-bilayer surfaces.

FIG. 2. FFM of a single-bilayer film of Cd arachidate (2×2 μm), acquired with an applied load of 6 nN. Total range of the topography in (a) is 240 Å, and that of the frictional force in (b) is 15 nN. An arrowhead-shaped structure is observable in the friction force map (b) which is not present in the topography image (a) [19]. The structure is interpreted as a material inhomogeneity, likely related to localized differences in coupling to the substrate.

sults in lower frictional forces of 0.2 nN. This observation demonstrates that the LB film acts as a lubricant on a microscopic scale. That the friction is lowered by about a factor of 10 on film-covered surfaces is in agreement with the magnitude of reduction observed on the macroscopic scale [2].

No difference in friction is measured between the two levels of the film (within an accuracy of 10%): the first and the second bilayer [Fig. 1(b)]. However, differences in friction are found *within* the organic film as inhomogeneities that are clearly observed in the friction force map but are not visible in the topography [19] [cf. arrowhead-shaped region in Fig. 2(b)]. In this particular film, with an applied normal force of 6 nN, the frictional force over these inhomogeneities is 0.9 nN, compared to 0.2 nN on the surrounding film and 3.5 nN on the substrate. The fact that these inhomogeneities are only observed on the single-bilayer films, and not on the double bilayers, indicates that they are likely due to interfilm or intrafilm coupling at the interface with the substrate. A more detailed investigation of the origins of these inhomogeneities is being pursued. Meanwhile, it is a significant and intriguing observation that these features

giving rise to frictional variations are *not* detectable in the normal topography mode.

An independence of frictional force on load has been observed at loads below a certain threshold. This has been noted on increasing the force from 1 to 10 nN, where only small changes in the frictional force on the LB films are measured, so the friction is taken, in a first approximation, to be constant, as shown in Fig. 3. This is in contrast to the previously cited study of a tungsten tip on graphite [6] in which frictional forces were found to be proportional to the applied normal force, in agreement with the classical Amonton's law which allows the determination of the friction coefficient. In the present case of low loads (1-10 nN), the frictional forces are nearly independent of the applied normal force, a behavior not yet reported in the literature on a microscopic scale. An explanation might be found in Eyring's model of boundary lubrication (discussed below) where, briefly, a function of the form

$$F_L = F_0 + \alpha F_n$$

[F_L is lateral (friction) force, F_0 is a constant, and F_n is the applied normal force] predicts this behavior in cases
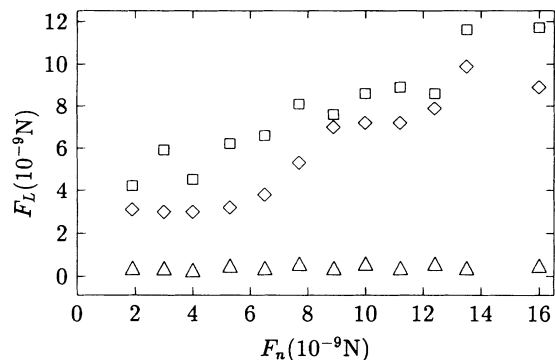
FIG. 3. Lateral forces F_L between probing tip and sample as a function of normal forces F_n. Data points are measured on the flat, film-covered areas ($\triangle$), at the step edges ($\square$), and on the substrate ($\lozenge$). The lateral forces at the step edges and on the substrate increase with load whereas these forces remain constant on the flat areas of the film.

FIG. 4. (a),(c) Topography images and (b),(d) friction force maps of a shearing event for a double-bilayer film of Cd arachidate (2×2 μm). Total range of the topography in (a),(c) is 240 Å, and that of the frictional force in (b),(d) is 14 nN. In (a),(b), with a 4-nN load, no damage is observed during the imaging. In (c),(d), with a 16-nN load, over the same area as in (a) and (b), the initial stage of wear is observed. Small islands and flakes are sheared away. The island indicated by the arrow in (a) is not observable in the final topography (c). In the friction force map (d) the lateral force to shear the particle is measured to be 5 nN.

when a, the proportionality constant, is small. This is the case with monolayers of fatty acids as determined in previous studies [20].

Wear processes start at forces above a threshold of ~ 10 nN, primarily at film edges. Before the onset of wear, it is already observed that the lateral forces are higher at the step edges than on the flat areas, ~ 8–12 and ~ 0.3 nN, respectively (cf. Fig. 3). This effect is attributed to the increase in contact area on impact with the edge of the upper bilayer and to nonideal force control at the step edges. If the normal force is increased, the lateral forces detected at the step edges are increased too (cf. Fig. 3).

Figures 4(a) and 4(b) are of an area on a bilayer film, imaged with a nondestructive load of 4 nN. Figures 4(c) and 4(d) are of the same area imaged with an increased force of 16 nN. Above a critical value of about 10 nN, small islands are moved in their entirety and particles are broken off the step edges. The sequence of images in Fig. 4 reveals, on close examination of the "before" and "after" topography of Figs. 4(a) and 4(c), several events of film modification, including removal of scattered islands and erosion of film edges.

In a representative shearing event, a particle of ~ 70 nm diameter is moved from the center of the image to beyond the top border [indicated with an arrow, Fig. 4(a)]. The pathway that this particle traverses is seen in the friction force image, Fig. 4(d), as it is successively moved along the surface of the film. The distinctly higher friction signal of this track reflects the increased lateral force required to shear the particle: 5 nN, compared to a measured lateral force of 0.3 nN over unperturbed, smooth film areas.

In a subsequent wide-area topographic scan (not shown), the sheared particle is found again. It is still of bilayer height, which demonstrates that the movement of these particles does not disrupt the ordered orientation of the molecules. From this observation an estimate of the
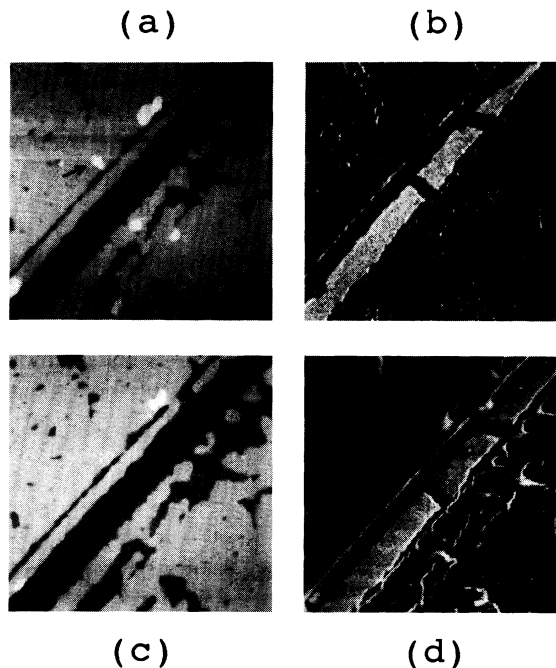
shear strength at the interface of the LB film in Fig. 4 can be made in the following manner. The contact area A is given by the geometrical dimensions of the sheared island; in the case of Fig. 4 the area is $A = 4900$ nm^2. The lateral force F_L to shear the island is 5 nN. A shear strength of $\tau = F_L/A = 1 \pm 0.2$ MPa is deduced.

Eyring's model of friction is applicable for approximating the shear of LB films against each other [21]. Here, the motion of a molecule or a group of molecules is restricted by the potential barrier due to its neighbors. The barrier can be overcome by stress τ or by random thermal fluctuations. As described in [20], shear stress τ is related to the normal pressure P and temperature T by

$$\tau = (k_B T/\Phi) \ln(v/v_0) + (1/\Phi)(Q' + P\Omega) ,$$

where k_B is the Boltzmann constant, v, v_0 are velocities with $v_0 = vb$, v a characteristic phonon frequency, and b the lattice constant, Q' is the height of the barrier, and Ω, Φ are stress and pressure activation volumes. The dependence on pressure originates from the pressure dependence of the barrier. The shear stress can be expressed in a short form by

$$\tau = \tau_0 + aP ,$$

with $\alpha = \Omega/\Phi$. In previous measurements with the SFA [20], monolayers of calcium stearate, deposited on mica sheets, were sheared across each other, yielding a value of $\tau_0 = 1$ MPa and $\alpha = 0.003$. For small loads these values are in good agreement with our observation. Actually, in the above AFM case of the sheared island, only interfacial forces act in the normal direction and the load is considered to be zero by definition.

The SFA measurements also showed that the pressure and stress activation volumes are larger than the volume of single molecules [20]. Therefore, it was hypothesized that the elementary shear mechanism is not the motion of individual molecules but the motion of blocks of molecules. This behavior is confirmed by the present AFM observation that the wear does not evolve continuously, but that wear starts at a critical force of 10 nN, shearing away small islands and flakes. Therefore, the collective motion of the molecules is preferred. The size of the sheared particles is determined by the applied shear stress.
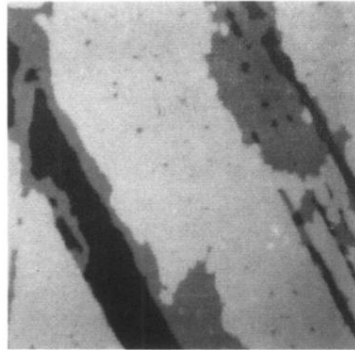
Our experiments show that the friction is roughly independent of the net forces in the regime of 1 to 10 nN, including both adhesive and externally applied forces. This is contrary to several schemes explaining the basic principles of boundary lubrication [22]. Among postulated factors, adhesion and elasticity have been suggested to be the relevant parameters. Reduced adhesion leads to smaller normal forces and may also influence the dissipation process of friction. LB films have rather small elasticities with a Young's modulus of 10 GPa [18], which is about a factor of 30 less than Si_3N_4. This soft material leads to a moderated strain distribution and reduces plastic deformation. Nonetheless, wear of the films is observed with the FFM at very low forces. Based upon the force microscope observations, we suggest that the unique properties of a boundary lubricant are not only low elasticity and adhesion but also the ability to conserve its local order on the molecular scale. Several processes can contribute to reach this aim: (1) The collective motion of molecules described above allows the rearrangement of the film with a minimum increase of disorder; and (2) amphiphilic molecules have the ability to reassemble via self-assembly (self-healing) [23]. Therefore, disruption of the film can be reversed on the molecular scale. Diffusion provides a degree of motion to the molecules, enabling the system to establish the lowest free energy configuration.

To conclude, it has been shown that friction force microscopy is well suited for studying the complex phenomena of boundary lubrication. The probing tip represents a single asperity and slides over the boundary lubricant. Wearless friction is observed for low forces. With higher forces the onset of wear is observed as a displacement of groups of molecules. The investigated LB films are very efficient in maintaining an ordered state. This characteristic, together with low friction, which minimizes local heating and inhibits melting, renders these amphiphilic films good boundary lubricants.
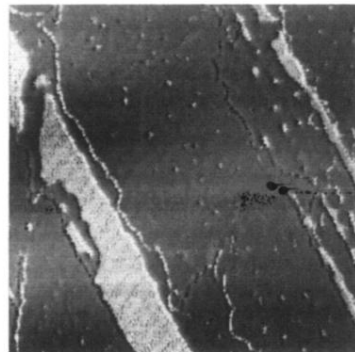
[1] E. Rabinowitz and D. Tabor, Proc. R. Soc. London A **208**, 455 (1951).
[2] A. I. Bailey and J. S. Courtney-Pratt, Proc. R. Soc. London A **227**, 501 (1954).
[3] G. Binnig, C. F. Quate, and C. Gerber, Phys. Rev. Lett. **56**, 930 (1986).
[4] For recent reviews see, e.g., D. Rugar and P. Hansma, Phys. Today **43**, No. 10, 23 (1990); J. Frommer and E. Meyer, J. Phys. Condens. Matter **3**, S1 (1991).
[5] G. Neubauer, S. R. Cohen, G. M. McClelland, D. Horne, and C. M. Mate, Rev. Sci. Instrum. **61**, 2296 (1990).
[6] C. M. Mate, G. M. McClelland, R. Erlandsson, and S. Chiang, Phys. Rev. Lett. **59**, 1942 (1987).
[7] M. Hirano, K. Shinjo, R. Kaneko, and Y. Murata, Phys. Rev. Lett. **67**, 2642 (1991).
[8] W. Zhong and D. Tomanek, Phys. Rev. Lett. **64**, 3054 (1990).
[9] U. Landman, W. D. Luedtke, N. A. Burnham, and R. J. Colton, Science **248**, 454 (1990).
[10] E. Meyer, L. Howald, R. M. Overney, H. Heinzelmann, J. Frommer, H.-J. Güntherodt, T. Wagner, H. Schier, and S. Roth, Nature (London) **349**, 398 (1991).
[11] L. Bourdieu, P. Silberzan, and D. Chatenay, Phys. Rev. Lett. **67**, 2029 (1991); D. Schwartz, J. Garnaes, R. Viswanathan, and J. Zasadinski (to be published).
[12] G. S. Blackman, C. M. Mate, and M. R. Philpott, Phys. Rev. Lett. **65**, 2270 (1990).
[13] For a detailed description of the preparation, see M. Schreck et al., Thin Solid Films **175**, 95 (1989).
[14] G. Meyer and N. M. Amer, Appl. Phys. Lett. **56**, 2100 (1990).
[15] O. Marti, J. Colchero, and J. Mlynek, Nanotechnology **1**, 141 (1990).
[16] The calibration procedure is to appear in a separate publication on instrumental aspects of friction force microscopy.
[17] K. L. Johnson, K. Kendall, and A. D. Roberts, Proc. R. Soc. London A **324**, 301 (1971).
[18] T. P. Weihs, Z. Nawaz, S. P. Jarvis, and J. B. Pethica, Ultramicroscopy (to be published).
[19] The faint shadowy outline of the arrowhead-shaped feature in the topography image, Fig. 2(a), is due to electronic coupling between the two channels (normal and lateral deflection) of the microscope.
[20] B. J. Briscoe and D. C. B. Evans, Proc. R. Soc. London A **380**, 389 (1981).
[21] H. Eyring, J. Chem. Phys. **3**, 107 (1935).
[22] S. M. Hsu, MRS Bull. **16**, No. 10, 54 (1991).
[23] J. Israelachvili, Intermolecular and Surface Forces (Academic, New York, 1991), 2nd ed.

FIG. 1. FFM of a double bilayer of Cd arachidate (2×2 μm), acquired with an applied load of 4 nN. (a) Topography of the film shows one- and two-bilayer steps, each bilayer with a height of 54 Å. The lowest level corresponds to the substrate. Total vertical range is 240 Å. (b) Friction force map shows increased friction on the substrate compared to the organic film. Total range in friction force in the map is 14 nN. No difference in friction is measurable between the single- and double-bilayer surfaces.
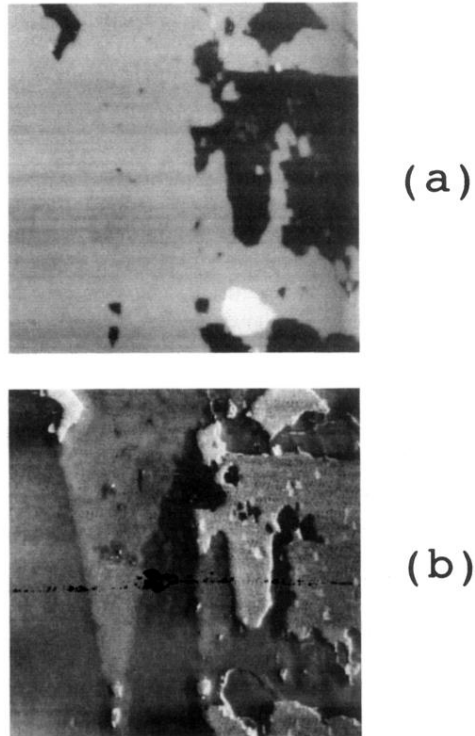
FIG. 2. FFM of a single-bilayer film of Cd arachidate (2×2 μm), acquired with an applied load of 6 nN. Total range of the topography in (a) is 240 Å, and that of the frictional force in (b) is 15 nN. An arrowhead-shaped structure is observable in the friction force map (b) which is not present in the topography image (a) [19]. The structure is interpreted as a material inhomogeneity, likely related to localized differences in coupling to the substrate.
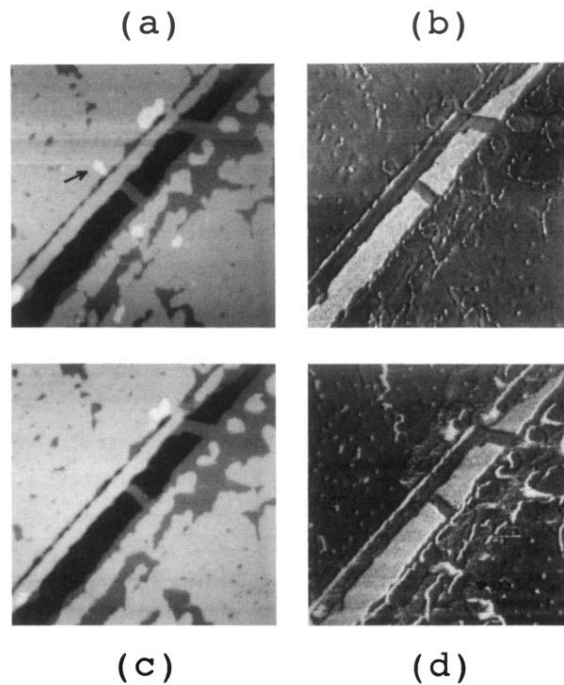
FIG. 4. (a),(c) Topography images and (b),(d) friction force maps of a shearing event for a double-bilayer film of Cd arachidate (2×2 μm). Total range of the topography in (a),(c) is 240 Å, and that of the frictional force in (b),(d) is 14 nN. In (a),(b), with a 4-nN load, no damage is observed during the imaging. In (c),(d), with a 16-nN load, over the same area as in (a) and (b), the initial stage of wear is observed. Small islands and flakes are sheared away. The island indicated by the arrow in (a) is not observable in the final topography (c). In the friction force map (d) the lateral force to shear the particle is measured to be 5 nN.